

Effect of Sand Sphericity and Cement-To-Sand Ratio on Effective Porosity and Permeability of Concrete Sand Filter

Gregorius Signer Pradana*, Budi Kamulyan, Intan Supraba

Department of Civil and Environmental Engineering, Faculty of Engineering, Universitas Gadjah Mada, Yogyakarta 55281, Indonesia

Keywords:
Cement-to-sand Ratio
Concrete Sand Filter
Effective Porosity
Hydraulic Properties
Sphericity

ABSTRACT

Sand filter is a widely used water treatment technology due to its operational simplicity. The drawbacks of sand filter operation are long backwash times and particle stratification, leading to high energy and sand replacement costs. The concrete sand filter (CSF) is created by mixing sand with cement paste as a binding agent. CSF establishes its water production capacity based on its effective porosity and permeability, which are influenced by the shape of the sand. CSF may have more spherical grains because the cement paste covers the sand. Previous studies have investigated the influence of the shape and size of aggregates on the porosity and permeability of porous concrete. This study investigates the effective porosity and permeability of CSF using various sand shapes and cement-to-sand (c:s) ratios, as well as changes in the shape of the sand grains used to construct the CSF due to mixing with cement paste. The sand shape was characterized by their circle ratio sphericity; the c:s ratios tested were 0, 1:6.4, and 1:8.6. All specimens are 10.9 cm in diameter and 20 cm in height. The water displacement method was employed to measure the effective porosity, while the constant head method was used to determine the permeability. The results indicate that when the circle ratio sphericity of the sand used to construct the filter increases, the effective porosity and permeability of filters decrease for all c:s ratios. Specimens with high cement content have lower effective porosity and permeability and show a strong linear relationship ($R^2 = 0.9555$ at c:s = 1:6.4).



This is an open access article under the [CC-BY](https://creativecommons.org/licenses/by/4.0/) license.

1. Introduction

Porous concrete is a permeable material that allows water to flow through it due to its pore paths formed by the usage of gap-graded or narrowly-graded aggregate. Cement paste serves as a binding agent, ensuring that the aggregates remain intact and do not disperse under water flow. The porosity of porous concrete ranges from 15% to 35%, and permeability between 0.14 cm/s and 1.22 cm/s [1]. The permeable properties of porous concrete suit the need for eco-friendly pavement for drainage and groundwater recharge [2].

Besides its application in environmentally friendly pavement, the permeable properties and stable granules of porous concrete offer potential for water purification filter development. The usage of finer aggregates has led to the creation of concrete sand filters as a new filtration technology [3] [4]. Concrete sand filter is an advancement

over conventional sand filter, with the addition of a certain amount of cement paste to bind the sand. This modification prevents particle stratification during backwashing, thereby ensuring a more stable filter's operational duration and production capacity [4] [5].

Pores between filter grains are crucial in filtration as they provide space to trap suspensions carried by water. However, not all pores in porous concrete and concrete sand filters serve this purpose. Pores connected at one or both ends are useful for storing suspensions. Furthermore, these open pore pathways allow water to flow, influencing the hydraulic properties of porous concrete, particularly permeability [6] [7] [8]. Permeability is affected not only by porosity but also by pore connectivity and the tortuosity of pore pathways [6]. These physical properties determine the pore structure inside the filter. A more accurate prediction of porous concrete's permeability can be obtained by understanding the pore structure of porous

*Corresponding author.

E-mail: gregoriusignerpradana@mail.ugm.ac.id

<https://dx.doi.org/10.21831/inersia.v20i2.76088>

Received July 12th, 2024; Revised January 13th, 2025; Accepted January 13th, 2025
Available online January, 31st 2025

concrete [9]. However, many studies focus only on open pores (or effective pores), which are easier to measure due to the complexity of methods determining tortuosity and connectivity [6] [10]. Generally, an increase in open pore pathways enhances permeability [6] [7] [9]. Porosity and permeability determine the water production capacity per unit area in one cycle of concrete sand filters [11].

Aggregate morphology affects the pore structure within the filter media [12]. A shape descriptor often used to describe aggregate shape is sphericity (ϕ), a ratio indicating how closely a particle's shape is to a perfect sphere. Sphericity values range from 0 to 1, where the sphericity value equal to 1 denotes a perfectly spherical shape. The addition of cement paste in the production of concrete sand filters might alter the morphology of sand grains, affecting the porosity and permeability of the filters and, as a result, the filter performance. This study aims to advance filtration technology by exploring the effect of sand shape (defined by sphericity) and cement-to-sand (c:s) ratio variations on the porosity and permeability of concrete sand filters, as well as how much they alter from conventional sand filters.

2. Methods

2.1 Material

This study used three types of sand, namely Progo Sand, Malang Sand, and Bali Sand. Progo Sand was chosen because of its abundance and ease of access from the research site in Yogyakarta. Malang Sand and Bali Sand are typical sands used in aquascape; both were selected based on their distinct visual shape compared to Progo Sand. Progo Sand is a volcanic sand deposit from Mount Merapi located in the higher reaches of the Progo River. Malang Sand is produced by crushing hardened lava with

a stone crusher machine. Bali Sand is a type of sand found on beaches, known for its higher salt concentration in water used to wash it than in freshwater. Figure 1 shows the particular sand types used in this study.

The sand was sieved to obtain grains ranging in size from 1 – 2 mm and then washed thoroughly. The washing process for Bali Sand involved measuring the salinity of the wash water until it reaches 0,2 ‰ or less, the salinity of freshwater. The selected grain size was based on observations that most spherical grains in Bali Sand fall within the 1 – 2 mm range, which was also used in studies by Triatmadja [4], Kamulyan [11], and Arviananda et al. [13].

2.2 Sphericity Measurement

True sphericity, as proposed by Wadell in 1932, refers to the ratio of the surface area of a sphere to the surface area of a particle with the same volume. A scanning method is required to accurately measure the true sphericity of individual particles [12] [14], of which the machine is not always available. The Krumbein-Sloss Chart, developed in 1963, is often used to estimate sphericity because of its practicality. However, the estimation is inaccurate due to subjective judgment, presenting a poor correlation with true sphericity. This study used circle ratio sphericity (ϕ_{cr}) to characterize the shape of the sand grains employed. Circle ratio sphericity is a two-dimensional sphericity proxy with a value equal to the ratio of the maximum inscribed circle diameter to the minimum circumscribed circle diameter in the particle projection. A study by Rorato et al. [14] found that circle ratio sphericity had the best correlation in random projection (Pearson correlation coefficient = 0.66) and the second best in maximum area projection (Pearson correlation coefficient = 0.72).

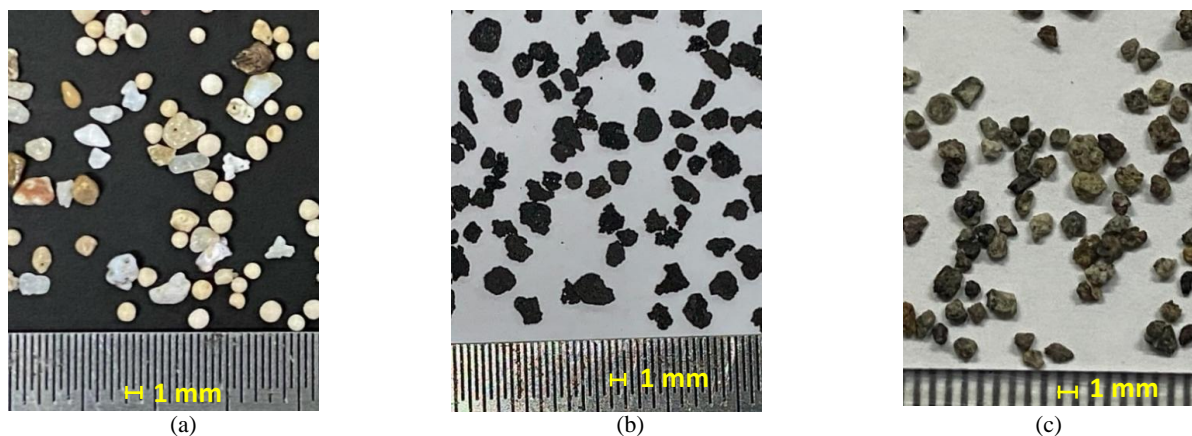


Figure 1. Sand used in the study: (a) Bali Sand, (b) Malang Sand, (c) Progo Sand

A small and random collection of sand samples was obtained by taking a pinch from each bag and mixing it in a container that has been rotated and shaken. The sand was rinsed thoroughly and placed in several 2 kg plastic bags. The sand grains were subsequently stretched on paper with contrasting color and photographed for ImageJ software processing.

The sand image was transformed to grayscale and binarized can be seen in Figure 2, and then the maximum inscribed circle diameter and minimum circumscribed

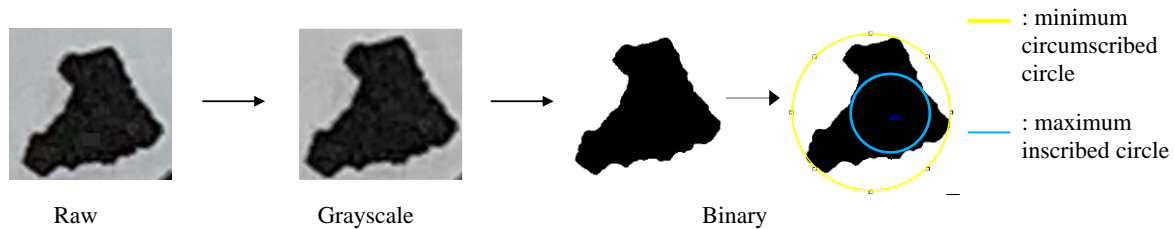


Figure 2. Image analysis of sand grains for circle ratio sphericity measurement

2.3 Concrete Sand Filter Specimens Production

The concrete sand filter specimens in this study were produced using three different types of sand and two ratios of cement-to-sand volume (denoted as c:s). A total of 18 concrete sand filter specimens were created, with three specimens for each sand type and c:s ratio combination. The specimens were molded in PVC molds with dimensions of 20 cm in height and 10.9 cm in diameter. This study utilized two c:s ratios to create specimens with varying cement additions: a lesser cement addition with a c:s = 1:8.6 and a higher cement addition with a c:s = 1:6.4. All specimens had a fixed water-to-cement ratio of 0.4. Table 1 shows the cement, sand, and water composition used to prepare the specimens, using the absolute volume method referred to by Yogafanny et al. [15]. The weights in Table 1 represent the material required for 1 m³ of mortar.

Concrete sand filters were made by mixing half the sand under saturated surface dry (SSD) conditions with cement for 2 minutes with a "Hobart" mixer. The remaining sand was added to the mixture and stirred for another 2 minutes to obtain a homogeneous mixture. Subsequently, water was slowly added to the mixture while it was constantly stirred for 2 minutes. The mixture was compacted once all of the ingredients have been thoroughly combined. Subsequently, the mixture was poured into a PVC mold set on a vibrating platform. The mixture was poured at half the mold's height during each step and compacted with a vibrator at the speed of 6 (out of 10) for 2 minutes. The

circle diameter were measured. Circle ratio sphericity is determined using Equation 1.

$$\phi_{cr} = \frac{d_{insc}}{d_{circ}} \quad (1)$$

where d_{insc} is the maximum inscribed circle diameter and d_{circ} is the minimum circumscribed circle diameter. Measurements were carried out for 1000 grains of sand of each type to obtain an overview of the distribution of sphericity values for each type of sand [14]. At this number of grains, the statistical parameter values begin to converge.

mold was then turned upside down and given one minute of additional compaction with a vibrator set to a speed of 5. If the mixture's height did not match the mold, more mixture was added and compacted at 5 for 1 minute. The compaction process was stopped when the mixture's height no longer decreases.

The concrete sand filter was cured 28 days before permeability and porosity tests were carried out. Curing was accomplished by wrapping the specimen in a gunny sack soaked every two days. Gunny sacks were chosen due to their ability to maintain water for a lengthy time, hence maintaining the humidity. This method was chosen rather than immersion to prevent the potential dissolution of the cement paste in water. Therefore, the porosity of the concrete sand filter remains relatively stable during the curing process.

2.4 Sand Filter Specimens Production

This study also utilized sand filters (without cement) compared to concrete sand filters. Sand filters were made with the same grain size, namely 1 – 2 mm, as concrete sand filters. Three specimens were prepared for each type of sand, resulting in nine specimens. The sand filter molds were constructed using PVC, measuring 20 cm in height and 10.9 cm in diameter. A 0.48 mm wire mesh was installed at the bottom of the molds to prevent sand from leaking out. The sand filter specimens were compacted using the same method as the concrete sand filter specimens.

Table 1. Mixture proportion of concrete sand filter

Sand Type	c:s	Material	Density (kg/m ³)	Absolute Volume Ratio	Absolute Volume of Dry Mortar* for 1 m ³ of Wet Mortar (m ³)	Weight of Materials (kg)
Progo Sand	1:6.4	Cement	3180**	1	0.18	571.54
		Sand	2614.78	6.4	1.15	3007.71
		Water	996	0.4	0.23	228.62
		Total		7.4	1.56	3807.87
		Unit weight (kg/m ³)				2441.67
	1:8.6	Cement	3180**	1	0.14	440.56
		Sand	2614.78	8.6	1.19	3115.41
		Water	996	0.4	0.18	176.23
		Total		9.6	1.51	3732.19
		Unit weight (kg/m ³)				2476.68
Malang Sand	1:6.4	Cement	3180**	1	0.18	571.54
		Sand	2438.66	6.4	1.15	2805.12
		Water	996	0.4	0.23	228.62
		Total		7.4	1.56	3605.27
		Unit weight (kg/m ³)				2311.76
	1:8.6	Cement	3180**	1	0.14	440.56
		Sand	2438.66	8.6	1.19	2905.56
		Water	996	0.4	0.18	176.23
		Total		9.6	1.51	3522.35
		Unit weight (kg/m ³)				2337.43
Bali Sand	1:6.4	Cement	3180**	1	0.18	571.54
		Sand	2153.95	6.4	1.15	2477.62
		Water	996	0.4	0.23	228.62
		Total		7.4	1.56	3277.78
		Unit weight (kg/m ³)				2101.77
	1:8.6	Cement	3180**	1	0.14	440.56
		Sand	2153.95	8.6	1.19	2566.34
		Water	996	0.4	0.18	176.23
		Total		9.6	1.51	3183.12
		Unit weight (kg/m ³)				2112.32

*1.33 m³ of dry mortar is needed to make 1 m³ of wet mortar [15]

**Based on Humaidi et al. [16] for pozzolan composite cement from Tiga Roda brand, which is the type of cement used in this study

2.5 Permeability Measurement

This study used the constant head method, as suggested by the study by Yogafanny et al. [15] on porous concrete for water filtration. The constant head method yielded more consistent findings than the falling head method.

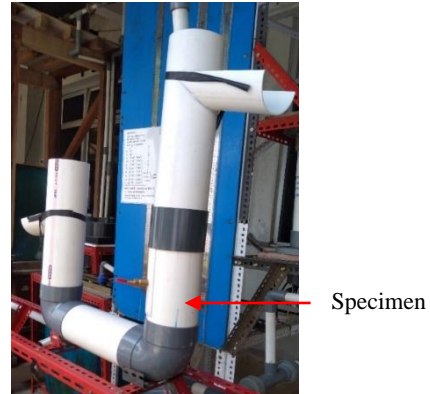
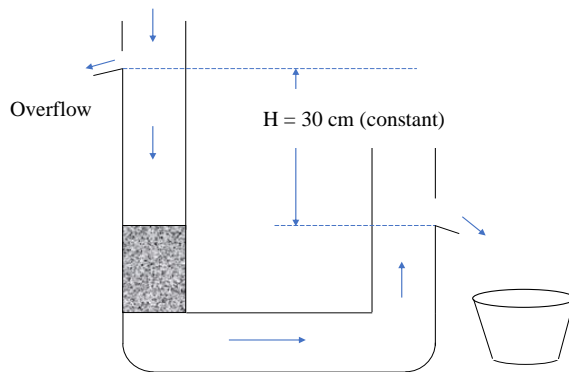


Figure 3. Permeability measurement scheme (left) and permeability measurement installation (right)

The permeability measurement with constant head method follows Darcy's law, calculated by Equation 2.

$$K = \frac{qL}{AHt} \quad (2)$$

where K is the permeability coefficient (cm/s), q is the volume of water collected (m^3) during t duration (s), A (cm^2) and L (cm) are the cross-sectional area and length of the specimen, respectively, H (cm) is the head difference which is kept constant at 30 cm. The water collection time of q cm^3 is 20 seconds.

2.6 Effective Porosity Measurement

The porosity assessed in this study is the effective porosity, which indicates the ratio of open pores to the bulk volume of the specimen. The specimens comprise solid fractions, open pores, and isolated pores in the concrete sand filter. The water displacement method was used to determine the effective porosity. The specimen was immersed in water, and the volume of water displaced by the immersion was measured. The rise in water level results from the displacement caused by the solid fraction. The volume of open pores is determined by subtracting the volume of water displaced by the solid fraction from the bulk volume of the specimen. Equation 3 is used to calculate the effective porosity:

$$\varepsilon_e = \frac{V_b - V_{dw}}{V_b} \times 100\% \quad (3)$$

The bulk volume (V_b) is the whole volume of the specimen, including the mold. V_{dw} represents the volume of water displaced by the solid fraction of the specimen. A similar method for measuring effective porosity on porous

concrete has been employed in studies conducted by Lian et al. [8] and Akkaya and Çağatay [17]. Furthermore, as stated by Sandoval et al. [7], the constant head method is able to capture differences resulting from the use of varying types of material. The constant head method also provides a shorter data-collecting time [15] and lower uncertainty [6]. Figure 3 shows the testing procedure and installation for measuring permeability.

concrete has been employed in studies conducted by Lian et al. [8] and Akkaya and Çağatay [17].

2.7 Statistical Test

Statistical testing was conducted to determine if the circle ratio sphericity (ϕ_{cr}) of each sand type exhibited a significant change following the addition of cement. Samples of 200 grains were collected from each type of sand and each variation of the cement-sand ratios (c:s). The ϕ_{cr} value was measured with ImageJ software, followed by a statistical permutation test using R software. The permutation test was chosen as a statistical test since it does not require data normality; however, if the data is normally distributed, the findings will be the same as those of the ANOVA test, which is more commonly used [18].

3. Result and Discussion

3.1 Circle Ratio Sphericity

Figure 4 shows the distribution of circle ratio sphericity (ϕ_{cr}) values obtained from measurements for three types of sand. Most Malang Sand grains have a ϕ_{cr} value that falls within the range of 0.5 to 0.7, with an average ϕ_{cr} value of 0.617. The ϕ_{cr} value of most Progo Sand grains falls within the range of 0.6 to 0.8, with an average ϕ_{cr} value of 0.682. The ϕ_{cr} value of most Bali Sand grains falls within the range of 0.8 - 1.0, with an average ϕ_{cr} value of 0.757. In contrast to Malang Sand and Progo Sand, Bali Sand consists of grains with quite diverse shapes, with very little variations in frequency over different ranges

shown in Figure 4. Bali Sand grains are found throughout a wide range of ϕ_{cr} values. Progo Sand and Malang Sand have grains with a more uniform shape, with the largest

concentration of ϕ_{cr} value lying between 0.6 – 0.8 and 0.5 – 0.7, respectively. The illustration of the grain shape is shown in Figure 5.

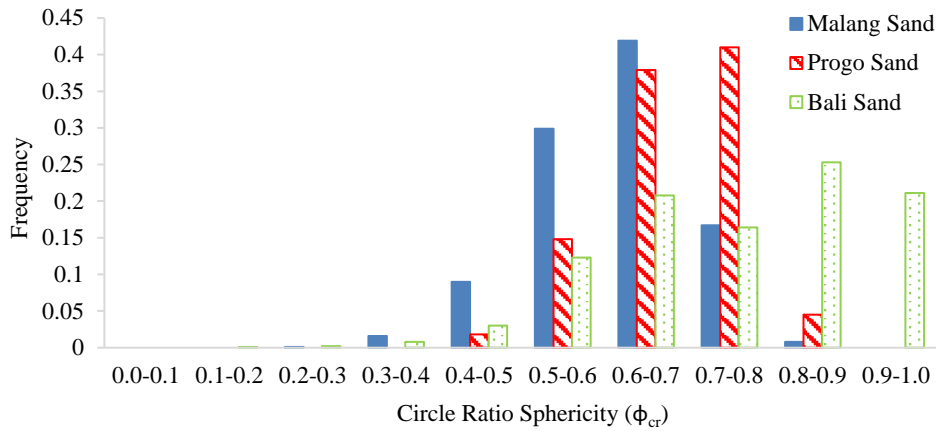


Figure 4. Distribution of circle ratio sphericity (ϕ_{cr}) value of each type of sand without cement addition

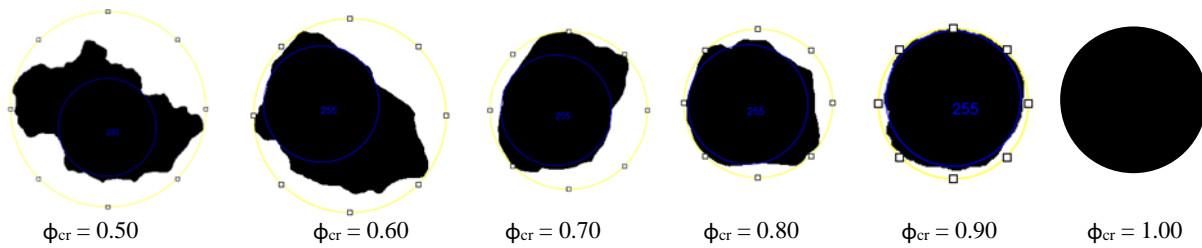


Figure 5. 2D illustration of sand grain shape at a given ϕ_{cr} value

The ϕ_{cr} values of sand grain samples in $c:s = 0$, $c:s = 1:8.6$, and $c:s = 1:6.4$ are shown in Table 2. Despite the dissimilar value compared to the average ϕ_{cr} before cement addition, the permutation test on the average ϕ_{cr} before and after cement addition indicate that only Malang Sand experienced a significant difference in ϕ_{cr} (p -value < 0.05) can be seen in Figure 6. Consequently, the Malang Sand grains have a somewhat more spherical shape after the addition of cement. Malang Sand grains derived from the

mechanical disintegration of lava stone are angular rich, resulting in bulges and depressions that make the cement that covers them difficult to remove. Progo Sand and Bali Sand did not significantly alter in shape due to their higher ϕ_{cr} values compared to Pasir Malang. As sphericity approaches 1, the surface grains become smoother [12]. The smooth surface makes it more difficult for the sand to remain encased by the cement paste, preventing significant changes in grain shape.

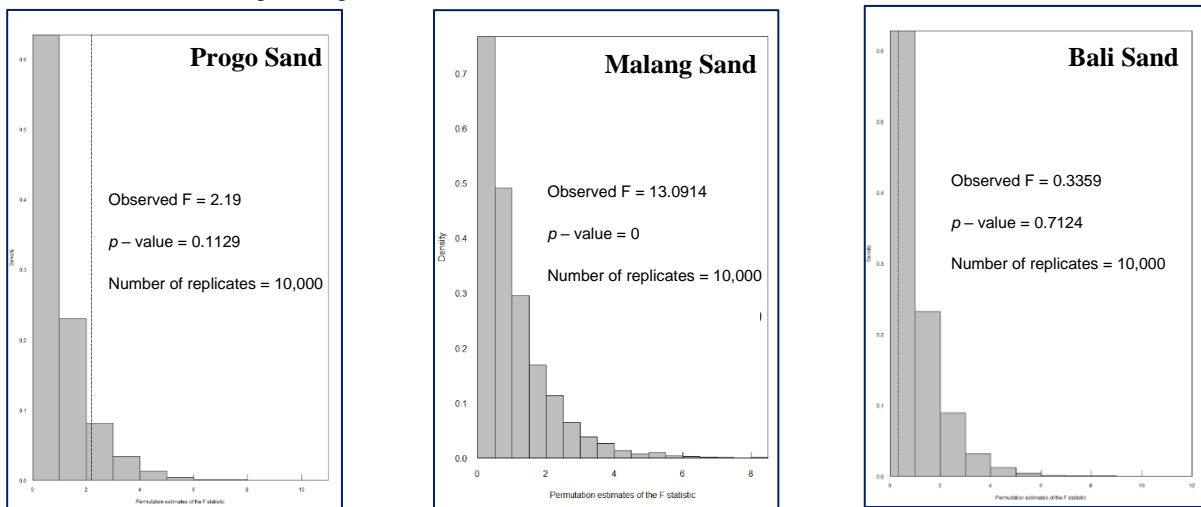


Figure 6. Permutation test results of average ϕ_{cr} before and after cement addition for each type of sand

Table 2. Value of ϕ_{cr} for each type of sand with cement-to-sand (c:s) ratio variations

c:s	Sand Type		
	Progo	Malang	Bali
1:6.4	0.711	0.661	0.764
1:8.6	0.693	0.648	0.756
0	0.682	0.617	0.757

3.2 Diameter of Grains

Figure 7 shows the distribution of grain diameters for each sand type. Bali sand has an effective size (ES) of 0.98 mm, a uniformity coefficient (UC) of 1.30, and grains that primarily have a diameter in the range of 1.1 – 1.2 mm. Progo sand has an ES of 0.94 mm, a UC of 1.32, and most of the grain diameters range from 1.1 to 1.2 mm. Malang sand is dominated by grains with a smaller diameter, namely 1.0 – 1.1 mm, has an ES of 0.91 mm and a UC of 1.40. These diameters refer to the diameter of the maximum inscribed circle measured using ImageJ from the projection of sand grain images. As the sand is sieved, the granules' positions will shift to the extent that they can eventually pass through the mesh. This phenomenon may result in sand grains passing through a mesh with a diameter lower than the minimum circumscribed circle size, as the maximum inscribed circle consistently has a diameter smaller than the minimum circumscribed circle.

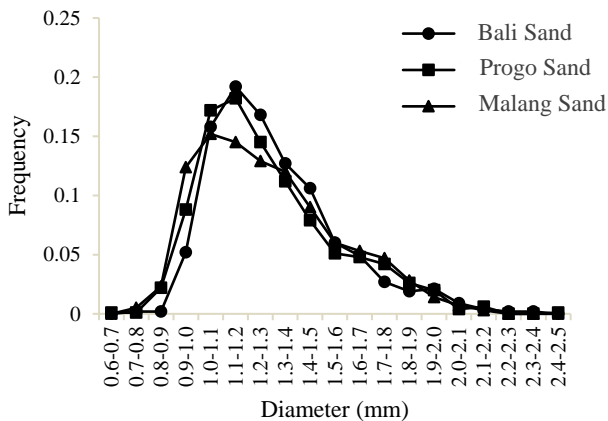


Figure 7. Grain Size Distribution for Each Type of Sand

3.3 Effective Porosity

Figure 8 shows the relationship between the circle ratio sphericity and the effective porosity for c:s = 0, c:s = 1:6.4, and c:s = 1:8.6. The highest effective porosity was found in sand filters with the lowest circle ratio sphericity. Conversely, the effective porosity decreases when the sand's circle sphericity ratio increases. Increasing the

amount of cement leads to a drop in the effective porosity of all types of sand. However, the sand with the lowest circle sphericity ratio still yields the highest effective porosity compared to the same variation in c:s. Wu et al. (2023) [12] discovered a similar phenomenon in which porosity decreases as the sphericity of the basalt aggregate employed increases. Conzelmann et al. (2022) [19] observed that the packing porosity of artificial aggregates in the shape of tetrapods, dolosse, and tetrahedra increased as sphericity decreased (sphericity < 0.92).

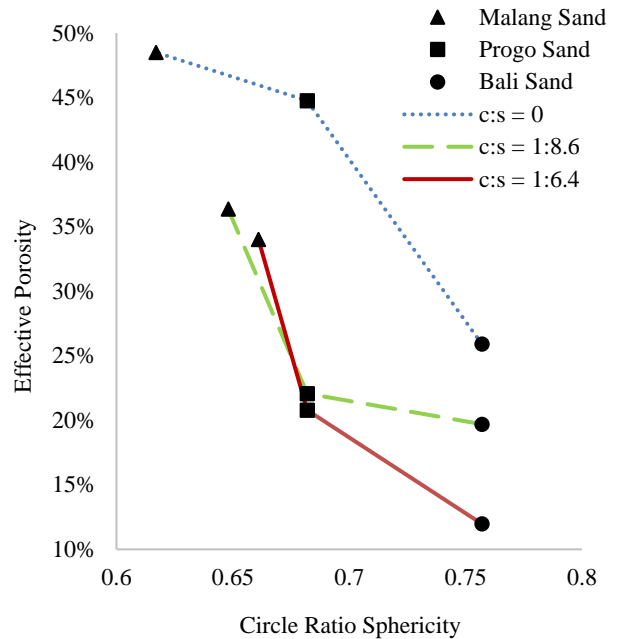


Figure 8. Effective porosity at different c:s ratios and circle ratio sphericity

Concrete sand filters made from Malang Sand with c:s = 1:6.4 have an average effective porosity of 34.02%. This value exceeds the average effective porosity of concrete sand filters made from Progo Sand with c:s = 1:8.6 at 22.08% and Bali Sand filters with c:s = 0 at 25.91%. The effective porosity of Malang Sand and Progo Sand filters drops dramatically from c:s = 0 to c:s = 1:8.6, by 12.14% and 22.67%, respectively, while the decline to c:s = 1:6.4 is relatively slight, at 2.34% and 1.30%, respectively. Filters constructed from Bali Sand exhibit a relatively consistent decrease in effective porosity, with a decrease of 6.21% (c:s = 0 to c:s = 1:8.6) and 7.72% (c:s = 1:8.6 to c:s = 1:6.4). Cement grains occupy the spaces between sand grains since they are far smaller than sand grains, which results in a decrease in porosity.

Compaction during the production stage affects the effective porosity of filters. During the compaction process, grains with low sphericity (meaning their shapes are more elongated and irregular) pose more significant

challenges for compaction. In contrast, grains with high sphericity (meaning they tend to be more spherical) are more easily compacted. Grains with a sphericity greater than 0.8 are nearly spherical, resulting in a minimal contact area between the grains. Consequently, the friction among grains decreases, facilitating easier compaction. Grains with an elongated shape (low sphericity) have higher friction because they have a greater contact area, resulting in more challenging compaction, especially if the grains are angularly rich since they have a high interlocking ability [12]. When grains are compacted easily, they generate fewer voids, while grains that are more difficult to compact generate more voids.

3.4 Permeability

Figure 9 shows the relationship between the circle ratio sphericity and the permeability of the filter for c:s = 0, c:s = 1:6.4, and c:s = 1:8.6. At the same level of cement addition, filters constructed from sand with low circle ratio sphericity produce high permeability. However, filter permeability drops when the circle ratio sphericity of the sand used to construct it increase. This relationship is similar to that of circle ratio sphericity and effective porosity. This is explicable since permeability is positively correlated with effective porosity [6] [9].

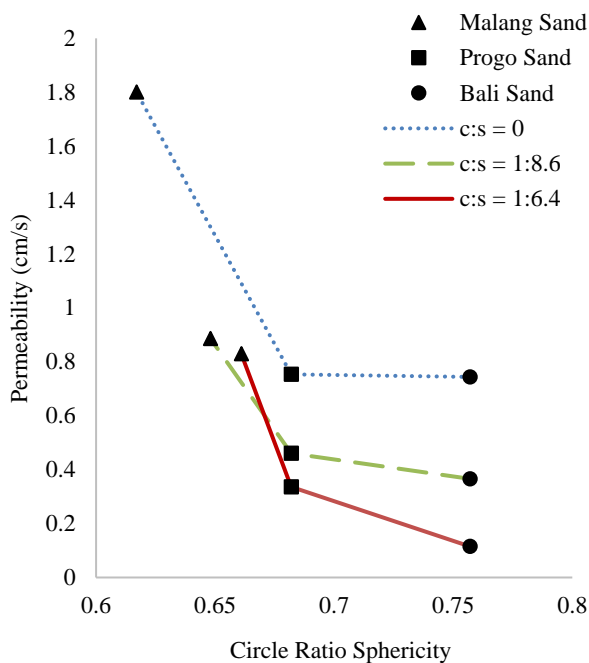


Figure 9. Permeability at different c:s ratios and circle ratio sphericity

The permeability of Malang Sand filters with a c:s of 1:6.4 is higher than those constructed from Progo Sand with a c:s of 0 and filters constructed from Bali Sand with a c:s

of 0, which are 0.83 cm/s, 0.75 cm/s, and 0.74 cm/s, respectively. The permeability of filters constructed from Malang Sand is decreased by 50.76% when the c:s ratio is increased from 0 to 1:8.6 and by 6.45% when the c:s ratio is increased from 1:8.6 to 1:6.4. Filters constructed from Progo Sand show a 38.93% decrease in permeability when the cement-to-sand (c:s) ratio is increased from 0 to 1:8.6, and a 27.00% decrease when the c:s ratio is altered from 1:8.6 to 1:6.4. The permeability of Bali Sand filters decreases by 50.80% when the c:s ratio is increased from 0 to 1:8.6, and by 68.53% when the c:s ratio is increased from 1:8.6 to 1:6.4.

The permeability of filters from each sand type decreases with an increased cement-sand ratio. At a higher cement-to-sand ratio, a portion of sand is replaced by cement compared to a filter with a lower cement-to-sand ratio. Cement possesses smaller particles, enabling it to occupy the empty spaces between sand grains. Consequently, the volume of interconnected pores, which serve as a channel for water flow, decreases. The rate of water flow per unit area decreases.

In addition to the growing number of interconnected pores, the rise in permeability could also be linked to differences in tortuosity for each type of sand employed. Conzelmann et al. [19] found that packing tortuosity increased as sphericity increased before a turning point in the trend occurred at a sphericity range of 0.81 – 0.92. On the contrary, tortuosity and permeability have a negative relationship [20] [21]. This phenomenon may be comprehended because when the tortuosity is significant, the distance water travels through the filter from the starting point to the endpoint increases. Consequently, the volume of water that travels through a filter with a larger tortuosity is less than that of a filter with a smaller tortuosity (shorter water path) during the same time.

3.5 Relationship Between Effective Porosity and Permeability of Concrete Sand Filters

Figure 10 illustrates the relationship between effective porosity (ϵ_{ef}) and permeability (K) for all concrete sand filter specimens. The power function correlation exhibited the highest correlation coefficient ($R^2 = 0.9301$) compared to the linear and exponential function. This finding is consistent with the relationship between effective porosity and permeability in porous concrete with coarser aggregate than concrete sand filter [22] [23]. Hou et al. [24] found a slightly lower R^2 for power function correlation (0.960) than exponential function correlation (0.962). Nevertheless, the power function is more accurate to predict the permeability of porous concrete (including

concrete sand filter) from their effective porosity than the simpler linear function.

The correlation between effective porosity and permeability will never attain a value of 1, indicating that permeability is not solely driven by effective porosity or there are factors other than effective porosity affect

permeability [6]. These other factors (such as tortuosity and pore throat size) collectively determine the pore structure characteristics of specimens. Porous concrete with identical porosity may not exhibit equivalent permeability due to potential variations in pore structure properties [12] [21].

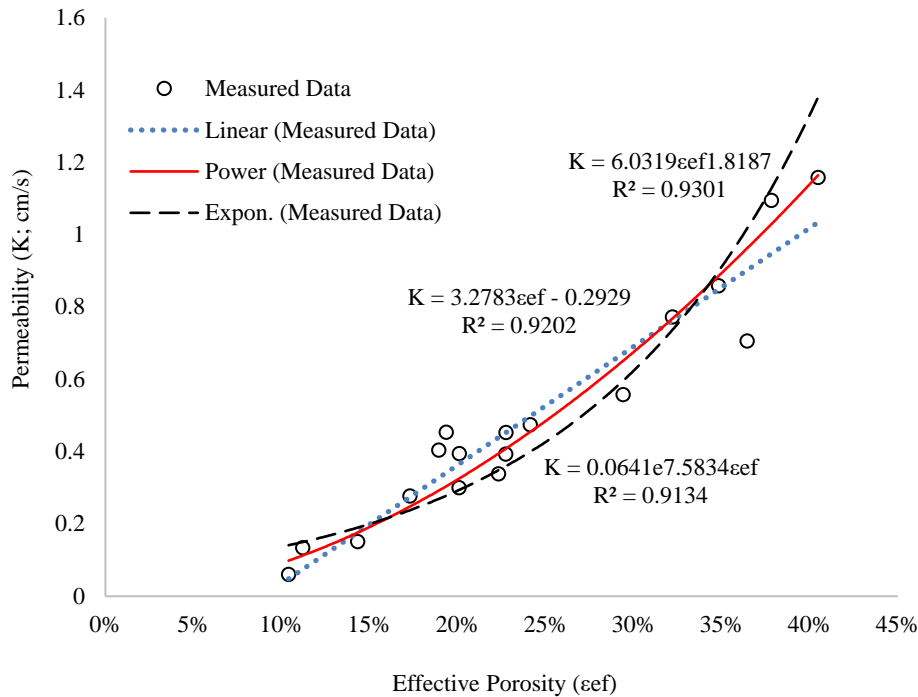


Figure 10. The relationship between effective porosity and permeability of concrete sand filters

4. Conclusion

The results of this study indicate that the effective porosity and filter permeability are negatively correlated with the circle ratio sphericity of the sand used to construct the filter, implying that the effective porosity and permeability of the filter decrease as the circle ratio sphericity of the employed sand increases. The following applies to all variations of the cement-to-sand ratio. The effective porosity and permeability are reduced when more cement is used. However, filters constructed from sand with a high circle ratio sphericity maintain lower effective porosity and permeability than those constructed from sand with a low circle ratio sphericity. The concrete sand filter specimens exhibited a strong power function correlation between effective porosity and permeability. Regarding the correlation between sand shape, effective porosity, and permeability, future study might be conducted to develop an equation for predicting effective porosity and permeability of permeable concrete based on their aggregate shape.

References

- [1] ACI 522R, "ACI522 - Pervious Concrete (PFE)," *American Concrete Institute*. 2010.
- [2] K. S. Elango and V. Revathi, "Infiltration and clogging characteristics of pervious concrete," *Asian Journal of Civil Engineering*, vol. 20, no. 8, pp. 1119–1127, 2019, doi: 10.1007/s42107-019-00170-w.
- [3] M. M. Taghizadeh, A. Torabian, M. Borghei, and A. H. Hassani, "A study of feasibility for water purification using vertical porous concrete filter," *International Journal of Environmental Science and Technology*, vol. 4, no. 4, pp. 505–512, 2007, doi: 10.1007/BF03325987.
- [4] R. Triatmadja, "Kajian Awal Prospek Filter Beton Pasir Sebagai Teknologi Tepat Filtrasi Air Bersih," *Prosiding Seminar Nasional Teknologi Tepat Guna Penanganan Sarana Prasarana Di Indonesia*, pp. 1–9, 2008.
- [5] B. Kamulyan, F. Nurrochmad, R. Triatmadja, and Sunjoto, "The Head Loss Development and Turbidity Removal of the Filtration using Concrete Sand Filter with Various Cement to Sand Ratio," *Proceeding of*

- the 4th ASEAN Environmental Engineering Conference*, pp. 17–20, 2011.
- [6] K. Seifeddine, S. Amziane, and E. Toussaint, “State of the art on the hydraulic properties of pervious concrete,” *Road Materials and Pavement Design*, vol. 24, no. 11, pp. 2561–2596, 2023, doi: 10.1080/14680629.2022.2164332.
- [7] G. F. B. Sandoval, I. Galobardes, R. S. Teixeira, and B. M. Toralles, “Comparison between the falling head and the constant head permeability tests to assess the permeability coefficient of sustainable Pervious Concretes,” *Case Studies in Construction Materials*, vol. 7, no. August, pp. 317–328, 2017, doi: 10.1016/j.cscm.2017.09.001.
- [8] C. Lian, Y. Zhuge, and S. Beecham, “The relationship between porosity and strength for porous concrete,” *Construction and Building Materials*, vol. 25, no. 11, pp. 4294–4298, 2011, doi: 10.1016/j.conbuildmat.2011.05.005.
- [9] D. Yavuz, Ş. Yazıcı, M. S. Avcı, and D. Özmen, “A novel approach to estimate the tortuosity of pervious concretes using computed tomography,” *Materials and Structures*, vol. 56, no. 4, 2023, doi: 10.1617/s11527-023-02166-0.
- [10] N. Neithalath, M. S. Sumanasooriya, and O. Deo, “Characterizing pore volume, sizes, and connectivity in pervious concretes for permeability prediction,” *Materials Characterization*, vol. 61, no. 8, pp. 802–813, 2010, doi: 10.1016/j.matchar.2010.05.004.
- [11] B. Kamulyan, “Karakteristik Hidraulik Filtrasi Dan Cucibalik Filter Beton,” Universitas Gadjah Mada, Yogyakarta, 2014.
- [12] S. Wu, Q. Wu, J. Shan, X. Cai, X. Su, and X. Sun, “Effect of morphological characteristics of aggregate on the performance of pervious concrete,” *Construction and Building Materials*, vol. 367, no. December 2022, p. 130219, 2023, doi: 10.1016/j.conbuildmat.2022.130219.
- [13] R. D. Arviananda, B. Kamulyan, and F. Nurrochmad, “Studies of Improving Drinking Water Quality in the Kalurahan Banaran Kabupaten Kulon Progo Using Porous Concrete Filter,” *INERSIA Informasi dan Ekspose Hasil Riset Teknik Sipil dan Arsitektur*, vol. 19, no. 2, pp. 194–202, 2023, doi: 10.21831/inersia.v19i2.64125.
- [14] R. Rorato, M. Arroyo, E. Andò, and A. Gens, “Sphericity measures of sand grains,” *Engineering Geology*, vol. 254, no. October 2018, pp. 43–53, 2019, doi: 10.1016/j.enggeo.2019.04.006.
- [15] E. Yogafanny, R. Triatmadja, F. Nurrochmad, and I. Supraba, “Permeability Coefficient of Pervious Cement Mortar Measured By the Constant Head and Falling Head Methods,” *Journal of Applied Engineering Science*, vol. 21, no. 4, pp. 1083–1093, 2023, doi: 10.5937/jaes0-44066.
- [16] M. Humaidi, K. Yanuar, A. Rafik, H. F. Agoes, R. A. Fajar, and Surat, “Variation of Cement Types Usage for Compressive Strength of Concrete Quality F’c 35 Mpa,” *Jurnal Multidisiplin Madani*, vol. 3, no. 3, pp. 773–788, 2023, doi: 10.55927/mudima.v3i3.2640.
- [17] A. Akkaya and İ. H. Çağatay, “Investigation of the density, porosity, and permeability properties of pervious concrete with different methods,” *Construction and Building Materials*, vol. 294, 2021, doi: 10.1016/j.conbuildmat.2021.123539.
- [18] D. R. Helsel, R. M. Hirsch, K. R. Ryberg, S. A. Archfield, and E. J. Gilroy, *Statistical Methods in Water Resources Techniques and Methods 4 – A3*. 2020. [Online]. Available: <https://pubs.er.usgs.gov/publication/tm4A3>
- [19] N. A. Conzelmann, M. N. Partl, F. J. Clemens, C. R. Müller, and L. D. Poulikakos, “Effect of artificial aggregate shapes on the porosity, tortuosity and permeability of their packings,” *Powder Technology*, vol. 397, 2022, doi: 10.1016/j.powtec.2021.11.063.
- [20] S. Ahmad, A. K. Azad, and K. F. Loughlin, “A Study of Permeability and Tortuosity of Concrete,” *30th Conference on OUR WORLD IN CONCRETE & STRUCTURES: August 23-24, 2005, Singapore*, no. August 2005, p. 9, 2005, [Online]. Available: <http://cipremier.com/100030015%5Cnwww.cipremier.com>
- [21] J. Shan, Y. Zhang, S. Wu, Z. Lin, L. Li, and Q. Wu, “Pore characteristics of pervious concrete and their influence on permeability attributes,” *Construction and Building Materials*, vol. 327, p. 126874, 2022, doi: 10.1016/j.conbuildmat.2022.126874.
- [22] L. Yang, S. Kou, X. Song, M. Lu, and Q. Wang, “Analysis of properties of pervious concrete prepared with difference paste-coated recycled aggregate,” *Construction and Building Materials*, vol. 269, p. 121244, 2021, doi: 10.1016/j.conbuildmat.2020.121244.
- [23] A. Abdelhady, L. Hui, and H. Zhang, “Comprehensive study to accurately predict the water permeability of pervious concrete using constant head method,” *Construction and Building Materials*, vol. 308, p. 125046, 2021, doi: 10.1016/j.conbuildmat.2021.125046.
- [24] F. Hou *et al.*, “Properties and relationships of porous concrete based on Griffith’s theory: compressive strength, permeability coefficient, and porosity,” *Materials and Structures*, vol. 57, no. 3, 2024, doi: 10.1617/s11527-024-02328-8.